The Journal of Experimental Biology 213, 3457-3462

doi:10.1242/jeb.043661

# Always on the bright side of life: anti-adhesive properties of insect ommatidia grating

Henrik Peisker* and Stanislav N. Gorb

Department of Functional Morphology and Biomechanics, Christian Albrecht University of Kiel, Am Botanischen Garten 1-9, D-24098 Kiel, Germany and Evolutionary Biomaterials Group, Max Planck Institute for Metals Research, Heisenbergstr. 3, D-70569 Stuttgart, Germany

*Author for correspondence (hpeisker@zoologie.uni-kiel.de)

Accepted 26 July 2010

## SUMMARY

**The surface of some insect eyes consists of arrays of cuticular protuberances, which are 50–300 nm in diameter, and are termed corneal nipples or ommatidia gratings. They were widely reported to reduce the reflectance for normally incident light, contributing to camouflage by reducing glare to predators, while furthermore enhancing the intake of light, which is especially important for nocturnal insects. Our preliminary observations suggest a third function: in contrast to the rest of the body, ommatidia of various insects remain clean, even in a heavy contaminated environment. In order to prove such an anti-contamination hypothesis of these structures, we measured the adhesive properties of polymer moulds of insect ommatidia, and compared these data with control surfaces having the same curvature radii but lacking such a nanostructure. A scanning electron microscope (SEM) study and force measurements using an atomic force microscope (AFM) on the eye surfaces of three different insect species, dragonfly *Aeshna mixta* (Odonata), moth *Laothoe populi* (Lepidoptera) and fly *Volucella pellucens* (Diptera), were undertaken. We revealed that adhesion is greatly reduced by corneal grating in *L. populi* and *V. pellucens* when compared with their smooth controls. The smooth cornea of *A. mixta* showed no statistically significant difference to its control. We assume that this anti-adhesive phenomenon is due to a decrease in the real contact area between contaminating particles and the eye's surface. Such a combination of three functions in one nanostructure can be interesting for the development of industrial multifunctional surfaces capable of enhancing light harvesting while reducing light reflection and adhesion.**

Key words: anti-adhesion, atomic force microscopy (AFM), contact area, ommatidia gratings, corneal nipples, insects, JKR model, scanning electron microscope (SEM).

## INTRODUCTION

The insect compound eye consists of 50 (*Xenos peckii*), 800 (*Drosophila melanogaster*) or even 10,000 (*Aeshna mixta*) individual eye facets (ommatidia), each with its own lens and a set of photoreceptor cells, packed in a hexagonal array. Compared with vertebrate camera-type eyes, insect compound eyes feature a large variation in the facet size and number and in corneal curvature. All these features contribute to a large variation in spatial resolution of the eye (Duparre and Wippermann, 2006). Insect eyes can detect fast movement (Olberg et al., 2007) and, in some cases, the polarisation of light (Labhart and Meyer, 1999). The biconvex, transparent and colourless corneal lens, partly consisting of resilin (Viswanathan and Varadaraj, 1985), forms the main part of the ommatidium cuticle and contributes to absorbing and filtering the suitable spectral range of light.

Surfaces of insect ommatidia contain nanoscale protuberances termed 'corneal nipples' or 'ommatidia gratings' (Bernhard and Miller, 1962; Miskimen and Rodriguez, 1981; Stalleicken et al., 2006). They are generally accepted to play a fundamental role in the anti-reflective properties of the optical system of the eye (Bernhard et al., 1965; Parker et al., 1998; Stavenga et al., 2006).

Eyes of many groups of pollinating insects, such as bees and flies, as well as eyes of subterranean beetles, may be negatively affected by pollen and dust contamination (Singer and Cocucci, 1997). However, a clean eye surface is crucial to the visually orientated insects. Our preliminary observations show that, in contrast to the rest of the body, ommatidia of various insects remain clean even in a heavy contaminated environment. In numerous insect species, the eye contamination problem is solved due to active cleaning systems (Hlavac, 1975; Jander, 1976). For example, highly elaborate grooming systems have been repeatedly reported in the literature for representatives of Hymenoptera (Schonitzer and Renner, 1984), Diptera (Szebenyi, 1969) and Coleoptera (Valentine, 1973).

By contrast, in addition to previously reported anti-reflection properties of ommatidial gratings, a self-cleaning mechanism based on cuticle geometry and surface energy is present on insect ommatidia. The principal aims of this study were to investigate (a) whether there is a significant variance in the adhesion properties between ommatidia of different insect species; (b) whether the variance in adhesion is due to a difference in surface topography; and (c) whether these structures could be biomimetically reproduced.

To investigate these aims, we measured the adhesive properties of insect ommatidia and of their polymer moulds, and compared these data with control surfaces that had the same curvature radii as ommatidia but lacked the nanostructure of corneal nipples. For this purpose, atomic force microscopy (AFM) was applied. It has been previously demonstrated that AFM is an excellent method to study the structure of insect surfaces at the highest resolution under near-living conditions and to evaluate surface adhesion properties (Voigt et al., 2009). The adhesive properties of ommatidia moulds of representatives from three different insect groups (Odonata, Lepidoptera and Diptera) were compared. While diurnal *Aeshna mixta* (Odonata) lacks protuberances, nocturnal *Laothoe populi* (Lepidoptera) and diurnal *Volucella pellucens* (Diptera) bear corneal nipples of different shapes.

## MATERIALS AND METHODS

### Insects and cornea preparation

The corneae of dead, dried dragonflies *Aeshna mixta* described by Pierre André Latreille 1805 (Odonata, Aeshnidae), moths *Laothoe populi* L.1758 (Lepidoptera, Sphingidae) and flies *Volucella pellucens* L.1758 (Diptera, Syrphidae) were taken from different collections and prepared using a scalpel and tweezers. The samples were rehydrated in aqua Millipore (Millipore GmbH, Schwalbach/Ts., Germany) for 10 min. For imaging, 3 mm×3 mm pieces of corneal cuticle were cut out and fixed on a glass slide using double-sided adhesive tape. Prior to and between measurements, all samples were kept in closed Petri dishes. Transparent corneae allowed their observation in an inverted light microscope (Zeiss Axiovert 135, Carl Zeiss MicroImaging GmbH, Göttingen, Germany) equipped with a AFM scanner head (JPK Instruments, Berlin, Germany). Due to the necessity of the sputter-coating procedure for scanning electron microscopy (SEM) and therewith an influence on the results of adhesion measurements, one (un-sputtered) cornea hemisphere of each insect was studied with AFM whereas the second hemisphere (sputtered) was used in SEM studies.

### Scanning electron microscopy

To gain additional information about the dimensions of the corneal nipples and to verify AFM images, a SEM Hitachi S-4800 (Hitachi High-Technologies Corp., Tokyo, Japan), operating at an accelerating voltage of 2 kV, was used. Samples were mounted on aluminium stubs using double-sided, carbon-containing, adhesive tape and were coated with gold–palladium (thickness 6 nm) in a Bal-tec SCD 500 Sputter Coater (Bal-tec AG, Balzers, Liechtenstein).

### Fabrication of cornea surface moulds

It is well known that surface chemistry influences the adhesive properties of the surface (Kendall, 2001). As different insect species and control surfaces have different surface chemistry, we were challenged to exclude the chemistry effect, in order to explore solely geometry effects, caused by ommatidia gratings, on adhesion. This is why we compared the adhesive properties not only of original insect ommatidia but also of resin moulds of compound eyes and those of control surfaces.

Negative moulds of the cornea samples, obtained using Affinis® dental wax (Coltène/Whaledent GmbH&Co. KG, Langenau, Germany), were subsequently moulded using epoxy resin, which was polymerised for 8 h at 70°C. We applied a low viscosity epoxy resin (Spurr, 1969), which is able to replicate even the smallest and rather complex biological surface features (Gorb, 2007).

To find smooth control surfaces with curvatures corresponding to those of the ommatidia, surface profiles (virtual cross-sections) of 10 randomly selected ommatidia of each insect species were obtained from AFM scans and averaged to obtain a mean curvature. The curvatures obtained for each insect species were then compared with the diameters of commercially available microspheres (Duke Scientific Corporation, Palo Alto, CA, USA), resulting in dimensions from 70 µm for *V. pellucens*, 140 µm for *L. populi*, up to 400 µm for *A. mixta*. These microspheres were used as templates to prepare smooth control surfaces with curvatures similar to that of ommatidia of the selected insect species. Spurr moulds of the control surfaces were fabricated as mentioned above.

### Atomic force microscopy

For imaging and adhesion measurements, we used a NanoWizard® atomic force microscope (JPK Instruments), mounted on an inverted light microscope (Zeiss Axiovert 135, Carl Zeiss MicroImaging GmbH). The AFM intermittent contact mode was applied to visualise the corneal nipples of the insects. The error channel (also known as the amplitude channel) visualises the change in damping of the cantilever amplitude while scanning the surface. Only images obtained with the error channel are shown, because this visualisation method permits a better comparison with SEM micrographs and enables a more vivid imaging of the surface topography. The force–distance curves were obtained on the resin moulds of the biological surfaces and control surface moulds. Scans were carried out in air (room temperature 24°C, relative humidity 41%) at a 1 Hz scan rate and a resolution of 1024×1024 pixels with an intermittent contact mode cantilever (c=50 N m$^{-1}$, NST-NCHF, Nascatec GmbH, Stuttgart, Germany). NanoWizard® SPM software 3.3.23 (JPK Instruments) was used to obtain AFM images. NanoWizard® image processing software 3.3.25 was applied to extract 3-D surface profiles and adhesive forces measured on each surface.

### Adhesion measurements

Adhesion measurements were carried out in air using a low frequency, non-contact mode cantilever (NST-NCLF) with a 30 µm certified traceable size standard sphere (Duke Scientific Corporation) attached to the cantilever tip. The spring constant of the cantilever (30 N m$^{-1}$) was ascertained using the thermal noise method (Hutter and Bechhoefer, 1993), before the sphere was attached to it.

On eyes of each of the three insect species studied, 10 ommatidia were chosen for adhesion measurements. To prevent a double contact of the sphere with two adjacent ommatidia, a 10 µm×10 µm scan pattern (force map) on top of each ommatidium was defined. Adhesion force measurements were carried out on these 100 selected sites within the 100 µm$^2$ area on each ommatidium. Adhesion force values of each of the 10 ommatidia were then averaged and statistically compared with the values obtained for the smooth control surface moulds. In all, 1000 individual force–distance curves for eyes of each insect species were collected and analysed.

### Contact area calculation

To calculate the nominal contact area between cantilever sphere and ommatidia moulds, the JKR contact model (Johnson et al., 1971), describing an adhesive contact between two spheres, was used. In the JKR model, the radius of the contact area ($a_0$) is given by:

$$a_0 = \left( \frac{12\pi\gamma R^2}{K} \right)^{\frac{1}{3}}, \quad (1)$$

where $\gamma$ is the surface energy, $K$ is the reduced stiffness and $R$ is the relative curvature radius, which is given by:

$$R = \frac{R_1 R_2}{R_1 + R_2}, \quad (2)$$

where $R_1$ is the ommatidium radius when extrapolated (from the measurements of AFM surface profiles) to a full sphere; $R_2$ is the radius of the sphere attached to the cantilever. $K$ from Eqn 1, implying the reduced stiffness, is related to the Young's modulus by:

$$K = \left( \frac{3}{4} \left[ \frac{1-\nu_a^2}{E_a} + \frac{1-\nu_b^2}{E_b} \right] \right)^{-1}, \quad (3)$$

where $E_a$ and $\nu_a$ are the Young's modulus and the Poisson ratio of the sample, respectively. $E_b$ and $\nu_b$ are the same parameters for the

sphere attached to the cantilever tip. With Eqns 2 and 3 substituted into Eqn 1, $a_0$ can be calculated. While $a_0$ only gives the radius of the contact area, the sphere sample contact area $A_C$ is given by:

$$A_C = \pi a_0^2 . \quad (4)$$

Consequently, the pull-off force can be calculated as:

$$\mathbf{F}_{\text{pulloff}} = \frac{3}{2}\pi\gamma R . \quad (5)$$

## RESULTS

### Surface structures

The comparison of SEM and AFM images of insect corneal nipples (Fig. 1) revealed that the heights of the gratings ranged from 25±6 nm (*L. populi*) to 70±10 nm (*V. pellucens*), packed in a hexagonal manner, as are the ommatidia themselves. However, packing of the respective protuberances is rather dissimilar in *L. populi* and *V. pellucens*. Whereas *L. populi* perpetuates the hexagonally dense packing at the nanoscale, *V. pellucens*, on the contrary, features laterally distinct nipples with valley distances of about 40 nm.

While in *A. mixta,* a regular grating was absent, a surface roughness (r.m.s.=1.3 nm) was observed. The aspect ratio of single nipples ranged from 0.1 for *L. populi* to 0.32 in *V. pellucens* with a peak-to-peak distance of 260±10 nm (*L. populi*) and 200±10 nm (*V. pellucens*).

Resin moulds of original surfaces demonstrated their excellent quality (Fig. 2). Differences in protuberance shape were negligible, permitting usage of moulds for adhesion measurements. The sphere moulds, used as control samples, featured similar roughness as the ommatidium surface of *A. mixta*.

### Adhesion measurements

Pull-off forces measured on the moulds of ommatidia of *L. populi* and *V. pellucens* were significantly lower than those obtained on the smooth control surface moulds (Fig. 3). A statistically significant difference in pull-off force of ommatidia moulds (Mann–Whitney rank sum test, $P \geq 0.001$) for *L. populi* (77±13 nN) and *V. pellucens* (19±1 nN) was found when compared with their smooth control surface mould values (*L. populi* control: 0.9 µN and *V. pellucens* control: 1.9 µN). Values obtained for *A. mixta* ommatidia moulds (178±40 nN) and their control samples (1.2±0.5 µN) suggest a difference in adhesion, which could not be statistically verified. A comparison between obtained adhesion forces for each surface is given in Fig. 4.

### Calculation and visualisation of sphere–sample contact area

To calculate the real contact area between the ommatidium surface and the sphere attached to the AFM cantilever, the JKR model (Johnson et al., 1971) was used. With $R_1$ (radius of the sphere attached to the cantilever) kept constant at 30 µm and changing $R_2$, depending on the differing curvature values of the ommatidia known

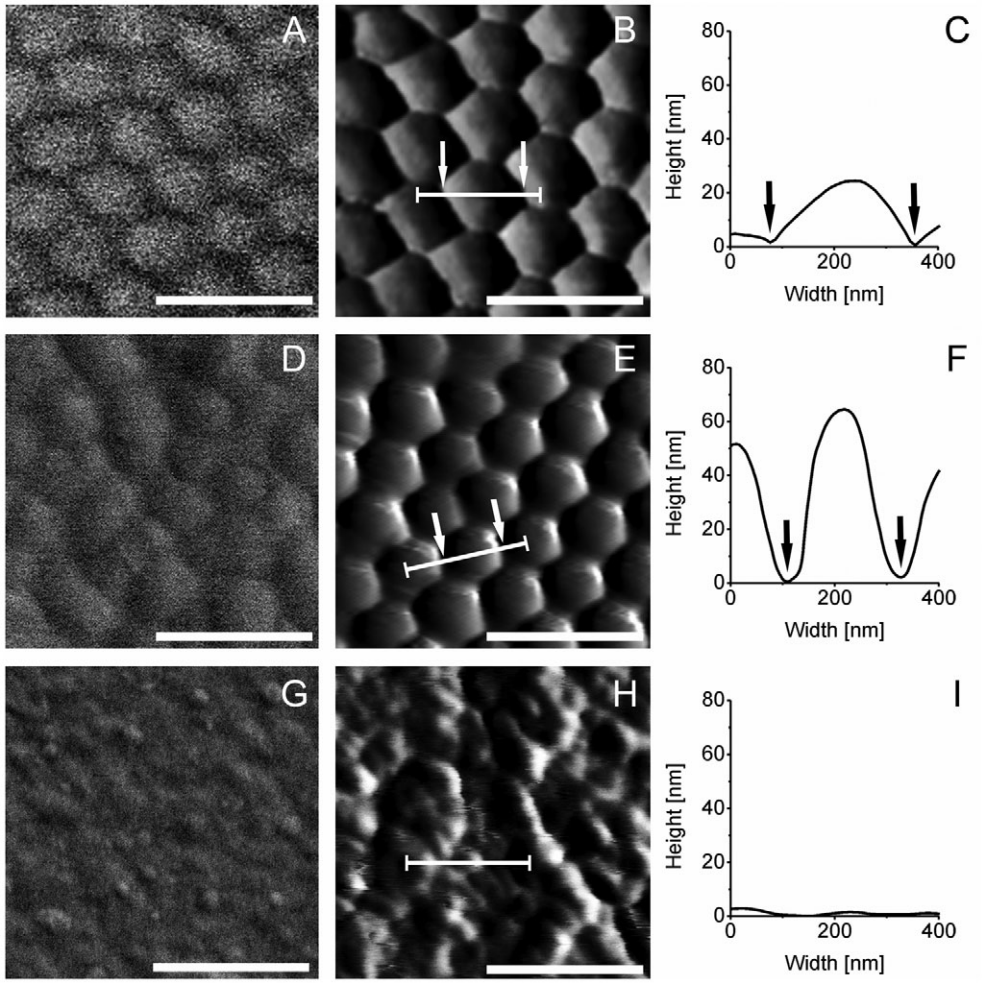


Fig. 1. Scanning electron microscopy (SEM) micrographs (A,D,G), atomic force microscopy (AFM) error channel images (B,E,H) and profiles (C,F,I) of corneal nipples from the moth *Laothoe populi* (first row), the fly *Volucella pellucens* (middle row) and the dragonfly *Aeshna mixta* (last row). White bars in B, E and H mark the area used for measurements of surface profile. The grating borders indicated by arrows in B, C, E and F correspond to the arrows shown in the surface profile diagrams. Scale bar in all images is 500 nm.

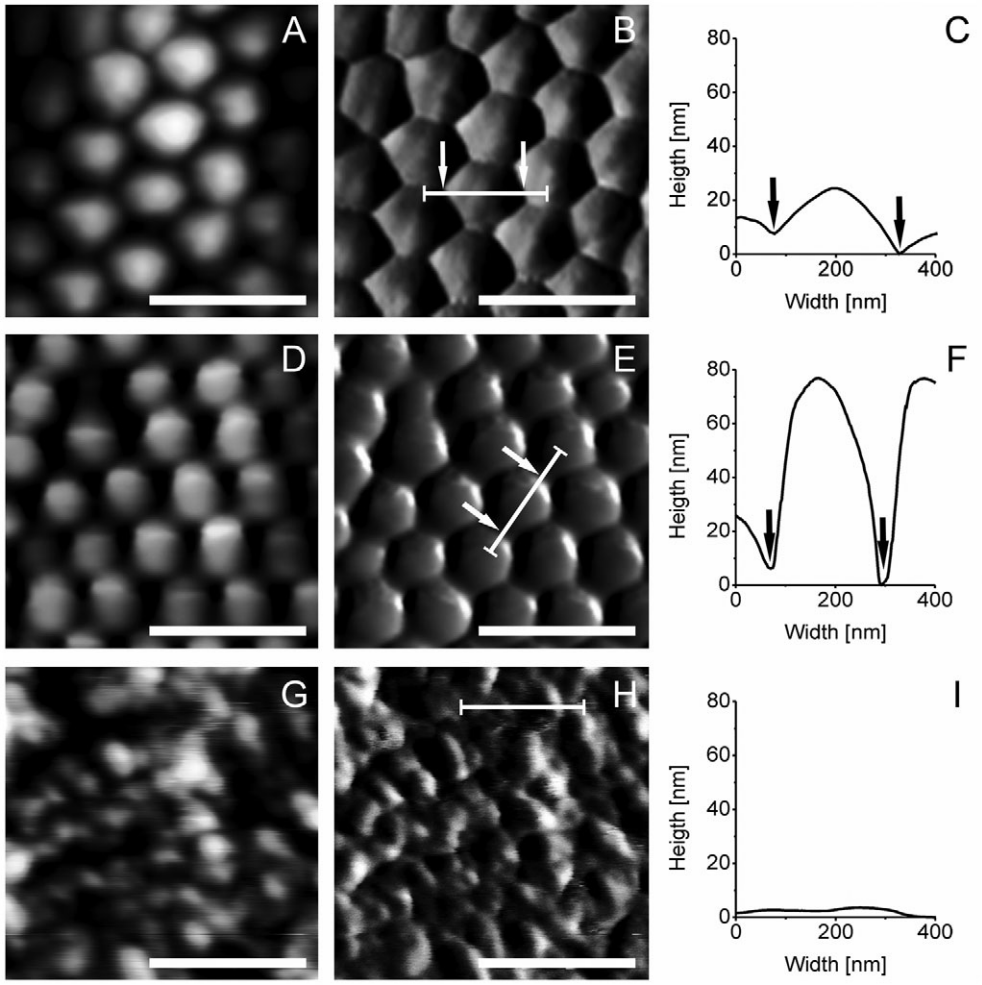


Fig. 2. Images from height (A,D,G) and error channels (B,E,H) of the atomic force microscopy (AFM) of three different insect corneal nipple moulds (first row: moth *Laothoe populi*; middle row: fly *Volucella pellucens*; last row: dragonfly *Aeshna mixta*) together with surface profile data (C,F,I). Arrows indicate protuberance borders depicted in the surface profile graphs. Scale bar is 500 nm.

from cross-section, Eqn 2 gives the reduced radius $R$ needed to determine contact radius $a_0$ (Eqn 1).

Reduced E-modulus $K$=11.3 GPa was derived for the equilibrium state from Eqn 3 by setting $E_a$=7 GPa (E-modulus of polymerised Spurr resin), $E_b$=70 GPa (E-modulus of glass) and Poisson ratios of both materials $\nu_a=\nu_b=0.5$. Substituting $R$, $K$ and $\gamma$=0.05 N m (Spolenak et al., 2005) in Eqn 1, $a_0$ is obtained. The $A_C$ can be calculated according to Eqn 4. Table 1 depicts the $R$, $a_0$ and $A_C$ values obtained for each type of surface–probe contact.

The relevant contact area for adhesion is further reduced, due to corneal grating within the calculated area of contact. Fig. 5 shows a visualisation of the calculated contact area (white circle) within an AFM error channel image of *L. populi*. It is clearly visible that only a few corneal nipples are able to make contact with the sphere whereas the rest of the calculated area remains untouched. For this reason, we recalculated the contact area and pull-off force, taking the number of possible contacts into account (Table 2).

## DISCUSSION

The data on topography and adhesion properties of the eyes of three different insect species, obtained in the present study, clearly demonstrate an anti-adhesive function of insect corneal protuberances. Our SEM and AFM images revealed that our measurements of *L. populi* and *V. pellucens* protuberance height and width and distribution of corneal nipples are in good agreement with previously published values (Bernhard and Miller, 1962; Bernhard et al., 1970). It is noteworthy that protuberance shape and packing density on the ommatidium surface are rather different in these two species, while *A. mixta* shows no grating at all. Whereas *L. populi* features a hexagonal close packing (h.c.p.) with a round and almost sphere-like

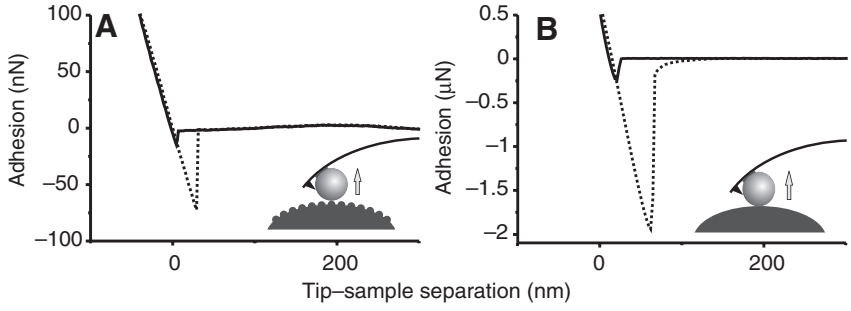


Fig. 3. Adhesion force comparison between a structured (A) and an unstructured surface (B) of *Laothoe populi*. Solid lines represent approach to the surface and dashed lines represent retraction. Both surfaces feature the same curvature but differ in nanoscale structuring. The contact area between the bead and the ommatidium is reduced due to the presence of such protuberances. Dimensions of the bead, nipples and ommatidia are not drawn to scale. Note the different scale dimensions in the diagrams.

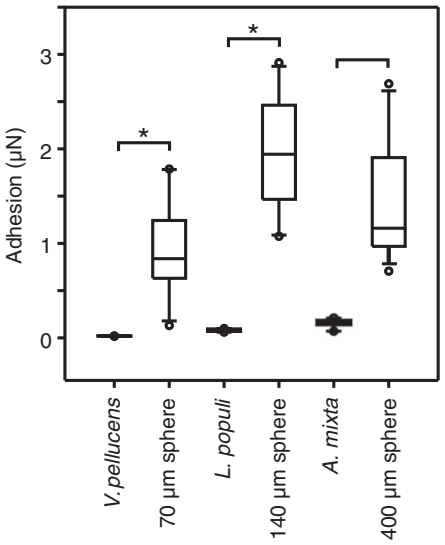


Fig. 4. Box-and-whisker plot of the measured adhesion forces of a 30 μm NIST sphere deposited on the cantilever and moulds of the species samples and their controls. Asterisks indicate a statistically significant difference in adhesion, which could not be found for *Aeshna mixta* and its corresponding control sample. The ends of the boxes define the 25th and 75th percentiles, with a line at the median and error bars defining the 10th and 90th percentiles (one-way ANOVA on ranks, $H_{5,10}$=53.141, $P$≤0.001).

Table 1. Comparison between the calculated relative ommatidium curvature radius $R$, contact radius $a_0$, contact area $A_C$ and pull-off force $\mathbf{F}_{\text{pull off}}$ for the ommatidia moulds of three sample species used and their controls, when interacting with the 30 μm sphere attached to the cantilever

| | *Aeshna mixta* | *Laothoe populi* | *Volucella pellucens* |
|---|---|---|---|
| Relative ommatidium curvature $R$ (μm) | 13.95 | 12.35 | 10.5 |
| Contact radius $a_0$ (μm) | 0.37 | 0.34 | 0.31 |
| Contact area $A_C$ (μm$^2$) | 0.43 | 0.36 | 0.30 |

Table 2. Comparison between the calculated pull-off force $\mathbf{F}_{\text{pull off}}$ for the ommatidia moulds and their controls, and the experimentally obtained values

| | *Aeshna mixta* | *Laothoe populi* | *Volucella pellucens* |
|---|---|---|---|
| Calculated $\mathbf{F}_{\text{pull off}}$ (nN) (control) | 3300 | 2900 | 2500 |
| Measured $\mathbf{F}_{\text{pull off}}$ (nN) (control) | 1200 | 1900 | 900 |
| Calculated $\mathbf{F}_{\text{pull off}}$ (nN) (ommatidia) | – | 90 | 23 |
| Measured $\mathbf{F}_{\text{pull off}}$ (nN) (ommatidia) | 178 | 77 | 19 |

Because the surface structure in *A. mixta* was very irregular, it was not possible to define the curvature radius of the structures and therefore calculate pull off according to JKR theory.

shape of nipples, *V. pellucens* shows a non-close packing (n.c.p.) and a more spike-like shape of single nipples. These two packing patterns were previously described for the mosquito *Culex pipiens* (Gao, X. F. et al., 2007). However, in *C. pipiens*, both patterns appear in the same individual and at different dimensions.

We found distribution and shape varieties in corneal grating correlated with measured adhesion. As aspect ratio increases, adhesion is reduced. The rather smooth, non-nippled ommatidia of *A. mixta* (r.m.s.=1.3 nm) demonstrated no statistical significant difference in adhesion when compared with their smooth control samples. Results obtained from the insect with smooth ommatidia emphasises the role of corneal grating in adhesion reduction.

It has previously been assumed that certain micro- and nanostructured surfaces, similar to the eye corneal grating, may be responsible for adhesion reduction between contaminating particles and biological surfaces, resulting in a self-cleaning property (Wagner et al., 1996). Literature data on other biological surfaces show that both surface structure and chemistry are involved in such a mechanism of anti-contamination (Barthlott and Neinhuis, 1997; Bhushan and Jung, 2008; Watson et al., 2008).

Numerous studies in the field of contact mechanics show a strong correlation between surface roughness and adhesion reduction due to a minimised area of contact between surfaces. It was found that a small surface roughness can completely remove adhesion (Kendall, 1971; Fuller and Tabor, 1975; Persson and Tosatti, 2001). Despite these findings, corneal grating has so far only been discussed with respect to super hydrophobicity (Gao, X. F. et al., 2007) or anti-reflective properties (Bernhard et al., 1965; Parker et al., 1998). In the present study, the remarkably low adhesion values were revealed on the ommatidia possessing corneal nipples, and the results of the calculations according to the JKR contact model lead to the conclusion that the real contact area in nippled ommatidia is reduced, when compared with the smooth ones. This means that the van der Waals forces, responsible for adhesion, may only occur on top of a few protuberances within the imaginary area of contact. The measured adhesion force is much lower compared with the mass of an average, for example, *Salvia glutinosa* pollen grain (0.041 μg), resulting in a non-sticky state. This phenomenon can also be applied to dust particles, etc. That is why the nippled ommatidia surfaces have self-cleaning properties mainly due to this particular hierarchical surface geometry. Additionally, during flight, wind drag and cuticle vibrations may contribute to the self-cleaning properties of the ommatidia.

One can assume that the presence of self-cleaning corneal surfaces may negatively correlate with the presence of structures actively used for grooming. As most insects strongly depend on their visual perception, which can be affected by contamination (Singer and Cocucci, 1997), some of them, like honeybees,

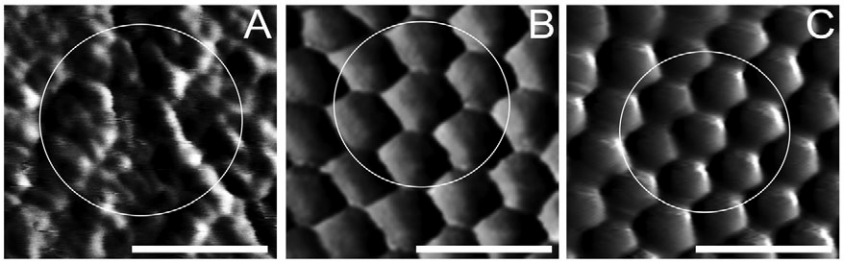


Fig. 5. Atomic force microscopy (AFM) error channel images depicting possible contact area (white circle) between a 30 μm NIST sphere positioned on the cantilever and the ommatidium of the dragonfly *Aeshna mixta* (A), the moth *Laothoe populi* (B) and the fly *Volucella pellucens* (C). Circle diameters are 740 nm (A), 640 nm (B) and 620 nm (C). Scale bars are 500 nm.

developed a highly elaborate cleaning device combined with grooming behaviour (Thorp, 1979), while in others, such as representatives of Lepidoptera, grooming is infrequently observed (Jander, 1976). This is why the lack of corneal grating may have pushed the development of more complex cleaning devices and corresponding grooming behaviour in some insect groups.

In conclusion, our observations of reduced adhesion due to ommatidia gratings and the results of our JKR model calculations of real contact area for different eye geometries indicate that the self-cleaning property of some insect eyes might be another biological function of ommatidia gratings in addition to their widely accepted anti-reflective properties and ability to reduce glare to predators. As our measurements on the polymer moulds of insect eyes show, such a strong anti-adhesive effect might be interesting for industrial applications. Corresponding technology for the development of surfaces having two hierarchical radii of curvature and simultaneously bearing self-cleaning and anti-reflective properties was recently described in the literature (Gao, H. J. et al., 2007).

## ACKNOWLEDGEMENTS

Sincere thanks to Christian Löbbe (JPK Instruments, Berlin, Germany) for his permanent support and help in the experimental setup. Valuable discussions with Lars Heepe on contact mechanics are acknowledged. This work, as part of the European Science Foundation EUROCORES Programme FANAS was supported from funds by the German Science Foundation DFG (contract No. GO 995/4-1) and the EC Sixt Framework Programme (contract No. ERAS-CT-2003-980409).

## REFERENCES

**Barthlott, W. and Neinhuis, C.** (1997). Purity of the sacred lotus, or escape from contamination in biological surfaces. *Planta* **202**, 1-8.
**Bernhard, C. G. and Miller, W. H.** (1962). A corneal nipple pattern in insect compound eyes. *Acta Physiol. Scand.* **56**, 385-386.
**Bernhard, C. G., Miller, W. H. and Moller, A. R.** (1965). The insect corneal nipple array: A biological, broad-band impedance transformer that acts as an antireflection coating. *Acta Physiol. Scand.* **63**, 1-79.
**Bernhard, C. G., Gemne, G. and Sallstro. J.** (1970). Comparative ultrastructure of corneal surface topography in insects with aspects on phylogenesis and function. *Z. Vergl. Physiol.* **67**, 1-24.
**Bhushan, B. and Jung, Y. C.** (2008). Wetting, adhesion and friction of superhydrophobic and hydrophilic leaves and fabricated micro/nanopatterned surfaces. *J. Phys. Condens. Matter* **20**, 1-24.
**Duparre, J. W. and Wippermann, F. C.** (2006). Micro-optical artificial compound eyes. *Bioinspir. Biomimet.* **1**, R1-R16.
**Fuller, K. N. G. and Tabor, D.** (1975). Effect of surface-roughness on adhesion of elastic solids. *Proc. R. Soc. Lond. A. Math. Phys. Sci.* **345**, 327-342.
**Gao, H. J., Liu, Z., Zhang, J., Zhang, G. M. and Xie, G. Y.** (2007). Precise replication of antireflective nanostructures from biotemplates. *Appl. Phys. Lett.* **90**, 123115.
**Gao, X. F., Yan, X., Yao, X., Xu, L., Zhang, K., Zhang, J. H., Yang, B. and Jiang, L.** (2007). The dry-style antifogging properties of mosquito compound eyes and artificial analogues prepared by soft lithography. *Adv. Mater.* **19**, 2213-2217.
**Gorb, S.** (2007). Visualisation of native surfaces by two-step molding. *Microsc. Today* **3**, 44-46.
**Hlavac, T. F.** (1975). Grooming systems of insects-structure, mechanics. *Ann. Entomol. Soc. Am.* **68**, 823-826.
**Hutter, J. L. and Bechhoefer, J.** (1993). Calibration of atomic-force microscope tips. *Rev. Sci. Instrum.* **64**, 1868-1873.
**Jander, R.** (1976). Grooming and pollen manipulation in bees (Apoidea): the nature and evolution of movements involving the foreleg. *Physiol. Entomol.* **1**, 179-194.
**Johnson, K. L., Kendall, K. and Roberts, A. D.** (1971). Surface energy and contact of elastic solids. *Proc. R. Soc. Lond. A. Math. Phys. Sci.* **324**, 301-313.
**Kendall, K.** (1971). Adhesion and surface energy of elastic solids. *J. Phys. D Appl. Phys.* **4**, 1186-1195.
**Kendall, K.** (2001). *Molecular Adhesion and its Applications: the Sticky Universe*. New York, NY: Kluwer Academic Publishing.
**Labhart, T. and Meyer, E. P.** (1999). Detectors for polarized skylight in insects: A survey of ommatidial specializations in the dorsal rim area of the compound eye. *Microsc. Res. Tech.* **47**, 368-379.
**Miskimen, G. W. and Rodriguez, N. L.** (1981). Structure and functional aspects of the Scotopic compound eye of the sugarcane borer moth. *J. Morphol.* **168**, 73-84.
**Olberg, R. M., Seaman, R. C., Coats, M. I. and Henry, A. F.** (2007). Eye movements and target fixation during dragonfly prey-interception flights. *J. Comp. Physiol. A* **193**, 685-693.
**Parker, A. R., Hegedus, Z. and Watts, R. A.** (1998). Solar-absorber antireflector on the eye of an Eocene fly (45 Ma). *Proc. R. Soc. Lond. B. Biol. Sci.* **265**, 811-815.
**Persson, B. N. J. and Tosatti, E.** (2001). The effect of surface roughness on the adhesion of elastic solids. *J. Chem. Phys.* **115**, 5597-5610.
**Schonitzer, K. and Renner, M.** (1984). The function of the antenna cleaner of the Honeybee (*Apis mellifica*). *Apidologie* **15**, 23-32.
**Singer, R. and Cocucci, A. A.** (1997). Eye attached hemipollinaria in the hawkmoth and settling moth pollination of Habenaria (Orchidaceae): a study on functional morphology in 5 species from subtropical South America. *Bot. Acta* **110**, 328-337.
**Spolenak, R., Gorb, S., Gao, H. J. and Arzt, E.** (2005). Effects of contact shape on the scaling of biological attachments. *Proc. R. Soc. Lond. A. Math. Phys. Sci.* **461**, 305-319.
**Spurr, A. R.** (1969). A low-viscosity epoxy resin embedding medium for electron microscopy. *J. Ultrastruct. Res.* **26**, 31-43.
**Stalleicken, J., Labhart, T. and Mouritsen, H.** (2006). Physiological characterization of the compound eye in monarch butterflies with focus on the dorsal rim area. *J. Comp. Physiol. A* **192**, 321-331.
**Stavenga, D. G., Foletti, S., Palasantzas, G. and Arikawa, K.** (2006). Light on the moth-eye corneal nipple array of butterflies. *Proc. R. Soc. Lond. B. Biol. Sci.* **273**, 661-667.
**Szebenyi, A. L.** (1969). Cleaning behaviour in *Drosophila melanogaster*. *Anim. Behav.* **17**, 641-651.
**Thorp, R. W.** (1979). Structural, behavioral, and physiological adaptations of Bees (*Apoidea*) for collecting pollen. *Ann. Mo. Bot. Gard.* **66**, 788-812.
**Valentine, B. D.** (1973). Grooming behavior in Coleoptera. *Coleopt. Bull.* 63-73.
**Viswanathan, S. and Varadaraj, G.** (1985). Occurrence of a resilin-like protein in the lens cuticle of the dragonfly *Mesogomphus lineatus* (Selys) (Anisoptera: Gomphidae). *Odonatologica* **14**, 155-158.
**Voigt, D., Peisker, H. and Gorb, S.** (2009). Visualization of epicuticular grease on the covering wings in the colorado potato beetle: a scanning probe approach. In *Applied Scanning Probe Methods XIII* (ed. B. Bhushan and H. Fuchs), pp. 1-16. Berlin, Heidelberg, New York: Springer.
**Wagner, T., Neinhuis, C. and Barthlott, W.** (1996). Wettability and contaminability of insect wings as a function of their surface sculptures. *Acta Zool.* **77**, 213-225.
**Watson, G. S., Myhra, S., Cribb, B. W. and Watson, J. A.** (2008). Putative functions and functional efficiency of ordered cuticular nanoarrays on insect wings. *Biophys. J.* **94**, 3352-3360.